HHS Public Access

Author manuscript

Nature. Author manuscript; available in PMC 2013 September 14.

Published in final edited form as:

Nature. 2013 March 14; 495(7440): 227–230. doi:10.1038/nature11926.

CXCL12 Production by Early Mesenchymal Progenitors is Required for Hematopoietic Stem Cell Maintenance

Adam Greenbaum[1,*], **Yen-Michael S. Hsu**[2,*], **Ryan B. Day**[1], **Laura G. Schuettpelz**[3], **Matthew J. Christopher**[1], **Joshua N. Borgerding**[1], **Takashi Nagasawa**[4], and **Daniel C. Link**[1]

[1]Department of Medicine, Washington University School of Medicine, St. Louis, MO, USA.

[2]Department of Pathology & Immunology, Washington University School of Medicine, St. Louis, MO, USA.

[3]Department of Pediatrics, Washington University School of Medicine, St. Louis, MO, USA.

[4]Department of Medical Systems Control, Institute for Frontier Medical Sciences, Kyoto University, 53 Kawahara-cho, Shogoin, Sakyo-ku, Kyoto 606-8507, Japan

Hematopoietic stem cells (HSCs) primarily reside in the bone marrow where signals generated by stromal cells regulate their self-renewal, proliferation, and trafficking. Endosteal osteoblasts[1,2] and perivascular stromal cells including endothelial cells[3], CXCL12-abundant reticular (CAR) cells[4,5], leptin-receptor positive stromal cells[6], and nestin-GFP positive mesenchymal progenitors[7] have all been implicated in HSC maintenance. However, it is unclear if specific hematopoietic progenitor cell (HPC) subsets reside in distinct niches defined by the surrounding stromal cells and the regulatory molecules they produce. CXCL12 (stromal-derived factor-1, SDF-1) regulates both HSCs and lymphoid progenitors and is expressed by all of these stromal cell populations[7–11]. Here, we selectively deleted *Cxcl12* from candidate niche stromal cell populations and characterized the effect on HPCs. Deletion of *Cxcl12* from mineralizing osteoblasts has no effect on HSCs or lymphoid progenitors. Deletion of *Cxcl12* from osterix-expressing stromal cells, which includes CAR cells and osteoblasts, results in constitutive HPC mobilization and a loss of B lymphoid progenitors, but HSC function is normal. *Cxcl12* deletion in endothelial cells results in a modest loss of long-term repopulating activity. Strikingly, deletion of C*xcl12* in nestin-negative mesenchymal progenitors using *Prx1-Cre* is associated with a marked loss of HSCs, long-term repopulating activity, HSC quiescence, and common lymphoid progenitors. These data suggest that osterix-expressing stromal cells comprise a distinct niche that supports B lymphoid progenitors and retains HPC in the bone

Correspondence: Daniel C. Link, Division of Oncology, Washington University School of Medicine, Campus Box 8007, 660 South Euclid Avenue, St. Louis, MO 63110, USA. dlink@dom.wustl.edu. Phone: 314-362-8771, Fax: 314-362-9333.

*These authors contributed equally to this work

Author Contributions

AMG and YMH designed and performed the research, analyzed the data, and wrote the manuscript. LGS, JNB, and RBD performed experiments characterizing hematopoiesis in the conditional *Cxcl12* deficient mice. MJC designed and cloned the CXCL12 conditional knockout construct. DCL supervised all of the research and edited the manuscript, which was approved by all co-authors. The authors have no conflicts of interest to disclose.

marrow, while expression of CXCL12 from stromal cells in the perivascular region, including endothelial cells and mesenchymal progenitors, support HSCs.

CXCL12 plays a crucial role in maintaining HSC function, including retention in the bone marrow[8,12–14], quiescence[15,16], and repopulating activity[16]. To test the hypothesis that CXCL12 production by different stromal cell populations has distinct effects on HSCs and lineage-committed HPC, we generated a floxed allele of *Cxcl12* (*Cxcl12*^{fl}) to conditionally delete *Cxcl12* from candidate niche cells in the bone marrow (Suppl. Fig. 2). Deletion of *Cxcl12* in endothelial cells and mature osteoblasts was mediated by the *Tie2-Cre* recombinase (*Cre*) and osteocalcin *(Oc)-Cre* transgenes, respectively. To target *Cxcl12* deletion in osteoprogenitors, we used the osterix *(Osx)-Cre* transgene, which mediates efficient recombination in mature osteoblasts and osteoblast progenitors[17]. It also targets CAR cells, a perivascular stromal cell population implicated in HSC and B lymphoid progenitor maintenance[5,11]. Finally, we used the *Prx1-Cre* transgene to target multipotent mesenchymal progenitors in the appendicular skeleton. Prx1 is a transcription factor expressed early during limb bud mesoderm development, and *Prx1-Cre* targets all cells derived from limb bud mesoderm[18]. Lineage mapping studies were performed using a *Cxcl12*^{gfp} knock-in mouse to define CAR cells[11]. These studies showed that both the *Osx-* and *Prx1-Cre* transgenes efficiently targeted recombination in mature osteoblasts, osteocytes, and CAR cells in long bones (Fig. 1a–d and Suppl. Fig 3).

Triple transgenic mice were generated containing one floxed *Cxcl12* allele, one null allele (*Cxcl12*$^{fl/-}$), and a *Cre*-recombinase transgene. Total CXCL12 mRNA expression in the femoral bone marrow of *Oc-* and *Tie2-Cre*-targeted mice was similar to that observed in control mice (Fig. 1e). In contrast, CXCL12 mRNA expression was reduced by 70% in *Osx-Cre*-targeted mice and nearly undetectable in *Prx1-Cre*-targeted mice. A similar decrease in CXCL12 protein levels was observed (Fig. 1f). To confirm *Cxcl12* deletion in CAR cells, mice containing *Cxcl12*$^{fl/gfp}$ and either the *Osx-* or *Prx1-Cre* transgenes, were generated (the *Cxcl12*^{gfp} allele is a null allele). Indeed, CXCL12 mRNA was nearly undetectable in CXCL12-GFP^{bright} CAR cells that were sorted from these mice (Fig. 1g). As expected, CXCL12 mRNA was nearly undetectable in endothelial cells sorted from *Tie2-Cre*-targeted mice (Fig. 1h). Together these data suggest that, under basal conditions, the majority of CXCL12 is produced by CAR cells, while mature osteoblasts and endothelial cells are only minor contributors.

All conditional knockout mice exhibited normal peripheral blood counts and the same relative percentage of granulocytes, monocytes, B cells, and T cells (Suppl. Table 1). However, bone marrow cellularity in femurs was reduced by approximately 50% in both the *Osx-Cre-* and *Prx1-Cre*-targeted mice, which was due, in part, to a loss of B cells. HPC subsets in the bone marrow were quantified by flow cytometry (Fig. 2a). The number of c-Kit^{+} Sca^{+} Lineage^{-} (KSL) cells, short-term HSCs, multipotent progenitors, and myeloid-committed progenitors was similar in all mice with the exception of a two-fold decrease in common myeloid progenitors in *Prx1-Cre*-targeted mice (Suppl. Fig. 4). Loss of CXCL12 expression in endothelial cells or mature osteoblasts had no effect on the number of phenotypic HSCs (Fig. 2 b–d). The frequency of phenotypic HSCs in the bone marrow of *Osx-Cre*-targeted mice was comparable to control mice (data not shown); however, since

bone marrow cellularity was reduced, a modest decrease in the absolute number of HSCs was observed. In contrast, a significant decrease in both the frequency and absolute number of phenotypic HSCs in *Prx1-Cre*-targeted mice was observed, with nearly undetectable dormant HSCs ($Flk2^{-}$ $CD34^{-}$ $CD150^{+}$ $CD48^{-}$ KSL cells). Consistent with these findings, competitive repopulation assays showed a significant multi-lineage long-term repopulating defect using bone marrow from *Prx1-Cre*- but not *Osx-Cre*-targeted mice (Fig. 3a–b). Despite the normal number of phenotypic HSCs, a small, but significant, decrease in long-term repopulating activity also was observed using *Tie2-Cre*-targeted bone marrow. Serial transplantation of bone marrow from *Prx1-Cre*- or *Tie2-Cre*-targeted mice showed no further decrease in repopulating activity in secondary recipients, suggesting that self-renewal capacity may be restored when HSCs are exposed to a normal stromal microenvironment (Suppl. Fig. 5). Quiescence is a fundamental property of HSCs, which is closely related to long-term repopulating activity[19]. Increased cycling of HSCs was observed in *Prx1-Cre*- but not *Osx-Cre*- or *Tie2-Cre*-targeted cells. In contrast, increased cycling of more mature KSL progenitors was observed in both *Prx1-Cre*- and *Osx-Cre*-targeted cells (Fig. 3c–d). Collectively, these data show that CXCL12 production from *Prx1-Cre*-targeted stromal cells and, to a lesser extent, endothelial cells is required for maintenance of HSC repopulating activity and quiescence. Consistent with results from the companion paper by Ding *et al.*, our data suggest that CXCL12 production from mature osteoblasts and osteoblast precursors is dispensable for HSC maintenance.

Since CXCL12 has been shown to play an important role in the retention of HPC within the marrow[5,20], we next quantified HPCs in the blood and spleen. In *Osx-Cre*-targeted mice, the number of colony-forming cells and KSL cells was increased in the blood and spleen, demonstrating constitutive HPC mobilization (Fig. 3e–f and Suppl. Fig. 6). Interestingly, though CXCL12 expression in the bone marrow is significantly lower, *Prx1-Cre*-targeted mice displayed a similar magnitude of HPC mobilization. Thus, our data suggest that, although CXCL12 production from *Osx-Cre*-targeted stromal cells is largely dispensable for HSC maintenance, it is required for the efficient retention of HPCs in the bone marrow.

CXCL12 is required for normal B and T cell development[19,21]. Pre-pro-B cells are found in close association with CAR cells[11], and ablation of CAR cells is associated with a loss of CLPs and pro-B cells[4]. Here, we show that deletion of *Cxcl12* in mineralizing osteoblasts or endothelial cells has no effect on CLPs, B lymphoid progenitors (BLPs), or pre-pro-B cells (Fig. 2e–h, Suppl. Figure 7). In contrast, *Cxcl12* deletion in CAR cells using *Osx-Cre* results in a marked loss of pre-pro B cells, and a trend towards a loss of BLP. However, CLPs and earliest thymic progenitors (ETPs) in the thymus are normal. Deletion of *Cxcl12* in *Prx1-Cre*-targeted stromal cells results in a similar phenotype but also results in a marked loss of CLPs. In the companion paper, Ding et al show that deletion of *Cxcl12* in osteoblasts using *Col2.3-Cre* also results in a modest decrease in CLP and lymphoid-primed multipotential progenitors (LMPP). Together, these data suggest that CXCL12 production from CAR cells or osteoblast precursors, but not mineralizing osteoblasts or endothelial cells, is required for the maintenance of B-lymphoid committed progenitors, while CLP maintenance is supported by CXCL12 production from both endosteal osteoblasts and a *Prx1-Cre*-targeted

perivascular stromal cell population. The normal CLP in *Osx-Cre*-targeted mice may be secondary to compensatory changes related to the severe loss of pre-pro-B cells.

We next performed studies to define the stromal cell population(s) differentially targeted by *Prx1-Cre and Osx-Cre*. We first considered the possibility that *Prx1-Cre* may target endothelial cells in the bone marrow. However, we detected no tdTomato expression in bone marrow endothelial cells from *Prx1-Cre* reporter mice (Fig. 4a–b). Moreover, expression of CXCL12 mRNA from sorted $CD31^+$ endothelial cells from *Prx1-Cre*-targeted mice was comparable to control mice (Suppl. Fig. 8). Thus, loss of CXCL12 from bone marrow endothelial cells does not account for the loss of HSCs in *Prx1-Cre*-targeted mice.

We extended the lineage mapping studies to the $CD45^-$ $lineage^-$ $PDGFR\alpha^+$ Sca^+ (PαS) cell population, which is enriched for mesenchymal stem cells[22]. Whereas *Osx-Cre* did not target this cell population, approximately 50% of cells were targeted by *Prx1-Cre*, including a subpopulation that expressed intermediate levels of CXCL12 (Fig. 4c–e). To evaluate the mesenchymal progenitor activity of the *Prx1*-Cre-targeted cells, we sorted *Prx1-Cre*-targeted ($tdTomato^+$) and non-targeted PαS cells and assessed their clonogenic capacity. All of the colony-forming unit-fibroblast (CFU-F) activity was contained with the *Prx1*-targeted PαS cell population, with greater than 10% of these cells having CFU-F activity (Fig 4f–g). This compares to a CFU-F frequency of approximately 4% in unselected PαS cells[22] and less than 1% in nestin-GFP^+ stromal cells[7]. The *Prx1*-targeted PαS cells have osteogenic and adipogenic differentiation potential *in vitro*, consistent with a mesenchymal stem cell phenotype (Fig 4h–i). RNA expression profiling of *Prx1*-targeted PαS cells is notable for the lack of nestin[7], CD146[9], or leptin receptor[6], all of which have been used to mark stromal cells contributing to HSC maintenance (Suppl. Table 2). Interestingly, other than moderate CXCL12 expression, these cells do not express genes classically associated with HSC maintenance, including kit ligand[6] and angiopoietin-1[19], though high expression of several matrix proteins (e.g., proteoglycan 4[23] and osteonectin[24]) implicated in HPC regulation is present.

Collectively, these data suggest that distinct stromal cell niches in the bone marrow exist that regulate specific HPC populations (Suppl. Fig. 1). Osterix-expressing stromal cells comprise a niche that supports B lymphoid progenitors and retains HPC in the bone marrow, while CXCL12 production from $nestin^-$ $leptin\ receptor^-$ mesenchymal progenitors is required for HSC and CLP maintenance.

METHODS SUMMARY

Targeting of the *Cxcl12* locus was accomplished by conventional techniques. Conditional knockouts were accomplished by interbreeding with *Osx-Cre*[25], *Prx1-Cre*[18], *Oc-Cre mice*[26], *Tie2-Cre*[27], and $Cxcl12^{+/-}$ mice[21]. Lineage mapping was accomplished using Ai9[28] and $Cxcl12^{gfp}$ mice[12]. All mice with the exception of $Cxcl12^{gfp}$ mice were maintained on the C56Bl6/J background. Unless indicated otherwise, data are presented as mean ± SEM and were analyzed with the Student's t-test, one-way ANOVA, or two-way ANOVA.

METHODS

Mice

With the exception of *Cxcl12*^{gfp} mice, all transgenic strains had been backcrossed at least 10 generations onto a C57BL/6 background. *Osx-Cre*[1], *Prx1-Cre*[2], *Tie2-Cre*[3], and Ai9 (B6.Cg-Gt(ROSA)26Sor$^{tm9(CAG-tdTomato)Hze}$/J)[4] mice were obtained from The Jackson Laboratory. *EIIa-Cre* mice[5] were a gift from Monica Bessler (University of Pennsylvania, Pennsylvania). *Oc-Cre* mice[6] were a gift from Thomas Clemens (Johns Hopkins University, Maryland), and *Cxcl12*^{gfp} mice[7] were a gift from Takashi Nagasawa (Kyoto University, Japan). *Cxcl12*$^{+/-}$ mice[8] were obtained through the RIKEN BioResource Center (Ibaraki, Japan). Mice were maintained under standard pathogen free conditions according to methods approved by the Washington University Animal Studies Committee.

Generation of *Cxcl12*^{fl} mice

A floxed allele of *Cxcl12* was generated containing *LoxP* sites flanking exon 2 of *Cxcl12*; a third *LoxP* was inserted 3' of the neomycin selection cassette (Suppl. Fig. 2). Generation of targeted embryonic stem cells and blastocyst injections were performed as previously described[9]. Excision of the neomycin cassette was accomplished through partial recombination by intercrossing mice with mice expressing *EIIa-Cre*. Mice were genotyped using PCR primers: *Cxcl12*^{flox} forward, 5'-CTACACCTCCTCTAGGTAAACCAGTCAGCC-3'; *Cxcl12*^{flox} reverse 5'-GGACACCAGAACCTTGAAACTGACA-3'.

Bone marrow transplantation

Bone marrow from WT *Ly5.1/5.2*-expressing mice was mixed at a 1:1 ratio with marrow from experimental or control mice expressing the *Ly5.2* locus. A total of 2×10^6 cells injected retro-orbitally into lethally irradiated (1,000 cGy) WT *Ly5.1*-expressing mice. Since Prx1 is expressed primarily in limb-bud derived long bones, only tibias and femurs were used for transplant and other analyses.

Blood, bone marrow, spleen, and thymus analysis

Blood, bone marrow, and spleen cells and thymocytes were harvested using standard techniques and quantified using a Hemavet automated cell counter (CDC Technologies).

Flow cytometry

Cells were stained by standard protocols with the following antibodies (eBiosciences unless otherwise noted): Lineage analysis and chimerism was assessed using peridinin chlorophyll protein complex (PerCP)-Cy5.5–conjugated Ly5.1 (A20, CD45.1), allophycocyanin (APC)-conjugated Ly5.2 (104, CD45.2), and one or more of the following lineage markers: APC-conjugated CD115 (AFS98, monocytes), fluorescein isothiocyanate (FITC)-conjugated Ly6C/G (RB6-8C5, Gr-1, myeloid), phycoerythrin (PE)-conjugated CD3e (145-2C11, T lymphocytes), and APC-eFluor780–conjugated CD45R (RA3-6B2, B220, B lymphocytes).

For HSPC analysis, cells were stained with a cocktail of biotin-conjugated B220, TER-119, CD3e, Gr1, and CD41 (MWReg30), PE-conjugated CD150 (TC15-12F12.2, Biolegend),

PE-Cy7-conjugated CD48 (HM48-1, BD Biosciences), PerCP-Cy5.5-conjugated Sca1 (D7), APC eFluor780-conjugated c-kit (2B-8), FITC-conjugated CD34 (RAM34), APC-conjugated Flk2 (A2F10), eFluor450-conjugated CD16/32 (93), and eFluor605NC-conjugated streptavidin. For HSC cell cycle staining, cells were stained with the biotin-conjugated lineage panel, PE-conjugated CD150, PE-Cy7-conjugated CD48, PerCP-Cy5.5-conjugated Sca, APC-conjugated c-kit, and APC-eFluor780-conjugated streptavidin. Cells were then fixed using the Cytofix/Cytoperm kit (BD Biosciences), stained with FITC-conjugated Ki-67 (B56, BD Biosciences), and resuspended in 1 mg/mL of 4',6-diamidino-2-phenylindole (DAPI). Doublets were gated out using FSC vs. FSC-W. Data were collected on a Gallios 10-color, 3-laser flow cytometer (Beckman Coulter). Data were analyzed with FlowJo (Treestar).

For CLP/BLP analysis, bone marrow cells were stained with a cocktail of PE-Cy7-conjugated B220, TER-119, CD3e, and Gr-1, APC-conjugated CD27 (LG.7F9), biotinylated IL-7Ra (gift of Deepta Bhattacharya, Washington University), PE-conjugated Flk2, FITC-conjugated Ly6D (49-H4, BD Biosciences), and eFluor450-conjugated streptavidin. CLP were defined as B220- TER-119- CD3e- Gr-1- CD27+ IL-7Ra+ Flk2+ Ly6D- cells, and BLP were defined as B220- TER-119- CD3e- Gr-1- CD27+ IL-7Ra+ Flk2+ Ly6D+ cells.

For Pre-pro B cell analysis, bone marrow cells were stained with APC-eFluor780-conjugated B220, a cocktail of PerCP-Cy5.5-conjugated CD3e, CD11c (N418), and NK1.1 (PK136), APC-conjugated IgM (II/4), eFluor450-conjugated IgD (11–26c), PE-Cy7-conjugated CD19 (eBio1D3), PE-conjugated CD43 (S7, BD Biosciences), and FITC-conjugated Ly6D (BD Biosciences). Pre-Pro B cells were defined as $B220^{+}$ $CD3e^{-}$ $CD11c^{-}$ $NK1.1^{-}$ IgM^{-} IgD^{-} $CD19^{-}$ $CD43^{+}$ $Ly6D^{+}$ cells.

For ETP analysis, thymocytes were stained using a cocktail of FITC-conjugated CD4 (RM4-5), CD8 (53-6.7), and CD11b (M1/70), a cocktail of PE-Cy7-conjugated B220, TER-119, CD3e, and Gr-1, PE-conjugated CD44 (IM7), eFluor450-conjugated CD25 (PC61.5), and APC-eFluor780-conjugated c-kit. ETP were defined as $CD4^{-}$ $CD8^{-}$ $CD11b^{-}$ $B220^{-}$ TER-119^{-} $CD3e^{-}$ $Gr^{-}1^{-}$ $CD44^{+}$ $CD25^{-}$ c-kit^{+} thymocytes.

Stromal cell analysis and sorting

To extract bone marrow stromal cells, intact bones were crushed in PBS by mortar and pestle. Crushed fractions in PBS were collected and stored on ice. The bone chips were digested using subjected to enzymatic digestion by collagenase type II (3mg/mL, Worthington Biochemical) and dispase (4mg/mL, Roche) at 37°C for 45 minutes at 37°C in a shaking water bath. Both crushed and digested fractions were pooled. Following RBC lysis, endothelial cells were stained with APC-conjugated CD45 (30-F11), FITC-conjugated lineage cocktail (CD3e, Gr-1, B220, and TER-119), and biotinylated anti-mouse CD31 (PECAM-1) followed by streptavidin PE. Dead cells were excluded using 7-AAD (EMD Biosciences). Perivascular mesenchymal progenitor cells were stained with APC-eFluor780-conjugated CD45 and APC-eFluor780-conjugated lineage cocktail, APC-conjugated Sca-1, biotinylated CD140a (PDGRFα), and streptavidin Brilliant Violet 421 (Biolegend). FACS analyses were performed using FACScan (BD Biosciences), LSRII (BD Biosciences), or Gallios (Beckman Coulter) flow cytometers. Cell sorting was done on Reflection (iCyt) or

Aria (BD Biosciences) flow cytometers. RNA of sorted cells was extracted using NucleoSpin RNA XS kit (Macherey-Nagel) per manufacture recommendations.

Quantitative RT-PCR

For total bone marrow RNA, femurs were flushed with 1 mL of Trizol (Invitrogen). RNA was prepared according to manufacturer's specification. One-step qRT-PCR was performed using the TaqMan Universal PCR Master Mix (Applied Biosystems) using no template and no RT controls. Data was collected on a 7300 Real-Time PCR System (Applied Biosystems). Primers were: CXCL12 forward, 5'-GAGCCAACGTCAAGCATCTG-3'; CXCL12 reverse, 5'-CGGGTCAATGCACACTTGTC-3'; CXCL12 dT-FAM/TAMRA probe, 5'-TCCAAACTGTGCCCTTCAGATTGTTGC-3'; β-actin forward, 5'-ACCAACTGGGACGATATGGAGAAGA-3'; β-actin primer; and β-actin dT-VIC/TAMRA probe, 5′-AGCCATGTACGTAGCCATCCAGGCTG-3′.

Immunofluorescence

Mice were lethally sedated and perfused with PBS followed by 4% paraformaldehyde. Hind limbs were removed and post-fixed in 4% paraformaldehyde overnight at 4°C. Bones were washed in water, decalcified in 14% EDTA pH 7.4, and cryoprotected in 30% sucrose in PBS. Bones were then snap frozen in OCT using liquid nitrogen-cooled 2-methylbutane, and blocks were sectioned at 7 μM. For lineage mapping, sections were washed in PBS and mounted with Prolong Gold Antifade Reagent with DAPI (Invitrogen). Slides were imaged using an ApoTome fluorescent microscope (Zeiss).

Colony-forming unit cell (CFU-C) assay

25,000 bone marrow cells or 50,000 spleen cells were plated in 2.75 ml methylcellulose media (MethoCult 3434; Stemcell Technologies). 20 μL of whole peripheral blood was RBC lysed and plated in methylcellulose. Duplicate cultures were incubated at 37°C for 7 days, after which colonies containing at least 100 cells were counted in a blinded fashion.

Colony-forming unit-fibroblast (CFU-F) assay

PDGFRα$^+$ Sca$^+$ cells were sorted by flow cytometry and directly plated on tissue culture plates containing alpha MEM and 10% fetal bovine serum (Atlanta Biologicals). Media exchanges were performed every 3–4 days for a total of 14 days, after which colonies containing at least 50 cells were counted. On day 14, cells were harvested from the cultures and replated in osteogenic or adipogenic media and cultured for an additional 14 days. Osteogenic media: alpha MEM with 10% fetal bovine serum, 50μM ascorbic acid (Sigma) and 10μM of β-glycerophosphate (Sigma). Adipogenic media: alpha MEM with 10% fetal bovine serum, 5μg/mL insulin, 100μM indomethacin, and 100nM dexamethasone. Osteoblast differentiation was assessed using the Leukocyte Alkaline Phosphatase Kit (Sigma), per manufacture's recommendations. Adipocyte differentiation was assessed by staining with Oil Red O, as reported previously[10].

RNA expression profiling

PDGFRα$^+$ Sca$^+$ cells or CAR cells, pooled from 2–6 mice, were sorted directly into lysis buffer and RNA was prepared using the RNA XS column kit (Macherey-Nagel, Bethlehem, PA) according to the manufacturer's directions. RNA was amplified using the NuGen Ovation system (NuGen, San Carlos, CA), and hybridized to the Affymetrix MoGene 1.0 ST array. Data normalization was performed using the Robust Multichip Average (RMA) algorithm. Submission of this RNA expression data to Gene Expression Omnibus is in progress.

Statistics

Significance was determined using Prism software (GraphPad). Unless otherwise stated, statistical significance of differences was calculated using 1- or 2-way ANOVA. P-values indicate the result of Bonferroni post-testing relative to *Cxcl12*$^{fl/-}$ control mice unless other comparisons are explicitly shown. P-values less than 0.05 were considered significant. All data are presented as mean ± SEM.

Supplementary Material

Refer to Web version on PubMed Central for supplementary material.

Acknowledgements

We thank Jill Woloszynek, Fulu Liu, Alex Khalaf, and Molly Romine for technical assistance; Gayle Callis, Stephen Oh, and Monica Vig for technical advice; Jackie Tucker-Davis for animal care, and Dr. Thomas Clemens for the *Oc-Cre* mice. This work was supported by NIH grants RO1 HL60772 (DCL) and F30 HL097423 (AMG).

REFERENCES

1. Calvi LM, et al. Osteoblastic cells regulate the haematopoietic stem cell niche. Nature. 2003; 425:841–846. [PubMed: 14574413]
2. Zhang J, et al. Identification of the haematopoietic stem cell niche and control of the niche size. Nature. 2003; 425:836–841. [PubMed: 14574412]
3. Hooper AT, et al. Engraftment and reconstitution of hematopoiesis is dependent on VEGFR2-mediated regeneration of sinusoidal endothelial cells. Cell Stem Cell. 2009; 4:263–274. [PubMed: 19265665]
4. Omatsu Y, et al. The essential functions of adipo-osteogenic progenitors as the hematopoietic stem and progenitor cell niche. Immunity. 2010; 33:387–399. [PubMed: 20850355]
5. Sugiyama T, Kohara H, Noda M, Nagasawa T. Maintenance of the hematopoietic stem cell pool by CXCL12-CXCR4 chemokine signaling in bone marrow stromal cell niches. Immunity. 2006; 25:977–988. [PubMed: 17174120]
6. Ding L, Saunders TL, Enikolopov G, Morrison SJ. Endothelial and perivascular cells maintain haematopoietic stem cells. Nature. 2012; 481:457–462. [PubMed: 22281595]
7. Mendez-Ferrer S, et al. Mesenchymal and haematopoietic stem cells form a unique bone marrow niche. Nature. 2010; 466:829–834. [PubMed: 20703299]
8. Peled A, et al. Dependence of human stem cell engraftment and repopulation of NOD/SCID mice on CXCR4. Science. 1999; 283:845–848. [PubMed: 9933168]
9. Sacchetti B, et al. Self-renewing osteoprogenitors in bone marrow sinusoids can organize a hematopoietic microenvironment. Cell. 2007; 131:324–336. [PubMed: 17956733]
10. Semerad CL, et al. G-CSF potently inhibits osteoblast activity and CXCL12 mRNA expression in the bone marrow. Blood. 2005; 106:3020–3027. [PubMed: 16037394]

11. Tokoyoda K, Egawa T, Sugiyama T, Choi BI, Nagasawa T. Cellular niches controlling B lymphocyte behavior within bone marrow during development. Immunity. 2004; 20:707–718. [PubMed: 15189736]
12. Ara T, et al. A role of CXC chemokine ligand 12/stromal cell-derived factor-1/pre-B cell growth stimulating factor and its receptor CXCR4 in fetal and adult T cell development in vivo. J Immunol. 2003; 170:4649–4655. [PubMed: 12707343]
13. Bonig H, Priestley GV, Nilsson LM, Jiang Y, Papayannopoulou T. PTX-sensitive signals in bone marrow homing of fetal and adult hematopoietic progenitor cells. Blood. 2004; 104:2299–2306. [PubMed: 15217839]
14. Kawabata K, et al. A cell-autonomous requirement for CXCR4 in long-term lymphoid and myeloid reconstitution. Proc Natl Acad Sci U S A. 1999; 96:5663–5667. [PubMed: 10318941]
15. Nie Y, Han YC, Zou YR. CXCR4 is required for the quiescence of primitive hematopoietic cells. J Exp Med. 2008; 205:777–783. [PubMed: 18378795]
16. Tzeng YS, et al. Loss of Cxcl12/Sdf-1 in adult mice decreases the quiescent state of hematopoietic stem/progenitor cells and alters the pattern of hematopoietic regeneration after myelosuppression. Blood. 2011; 117:429–439. [PubMed: 20833981]
17. Maes C, et al. Osteoblast precursors, but not mature osteoblasts, move into developing and fractured bones along with invading blood vessels. Developmental cell. 2010; 19:329–344. [PubMed: 20708594]
18. Logan M, et al. Expression of Cre Recombinase in the developing mouse limb bud driven by a Prxl enhancer. Genesis. 2002; 33:77–80. [PubMed: 12112875]
19. Arai F, et al. Tie2/angiopoietin-1 signaling regulates hematopoietic stem cell quiescence in the bone marrow niche. Cell. 2004; 118:149–161. [PubMed: 15260986]
20. Foudi A, et al. Analysis of histone 2B-GFP retention reveals slowly cycling hematopoietic stem cells. Nat Biotechnol. 2009; 27:84–90. [PubMed: 19060879]
21. Nagasawa T, et al. Defects of B-cell lymphopoiesis and bone-marrow myelopoiesis in mice lacking the CXC chemokine PBSF/SDF-1. Nature. 1996; 382:635–638. [PubMed: 8757135]
22. Morikawa S, et al. Prospective identification, isolation, and systemic transplantation of multipotent mesenchymal stem cells in murine bone marrow. J Exp Med. 2009; 206:2483–2496. [PubMed: 19841085]
23. Zhan M, Han ZC. Hemangiopoietin inhibits apoptosis of MO7e leukemia cells through phosphatidylinositol 3-kinase-AKT pathway. Biochemical and biophysical research communications. 2004; 317:198–204. [PubMed: 15047168]
24. Lehmann S, et al. Common deleted genes in the 5q- syndrome: thrombocytopenia and reduced erythroid colony formation in SPARC null mice. Leukemia : official journal of the Leukemia Society of America, Leukemia Research Fund, U.K. 2007; 21:1931–1936.
25. Rodda SJ, McMahon AP. Distinct roles for Hedgehog and canonical Wnt signaling in specification, differentiation and maintenance of osteoblast progenitors. Development. 2006; 133:3231–3244. [PubMed: 16854976]
26. Zhang M, et al. Osteoblast-specific knockout of the insulin-like growth factor (IGF) receptor gene reveals an essential role of IGF signaling in bone matrix mineralization. The Journal of biological chemistry. 2002; 277:44005–44012. [PubMed: 12215457]
27. Kisanuki YY, et al. Tie2-Cre transgenic mice: a new model for endothelial cell-lineage analysis in vivo. Developmental biology. 2001; 230:230–242. [PubMed: 11161575]
28. Madisen L, et al. A robust and high-throughput Cre reporting and characterization system for the whole mouse brain. Nat Neurosci. 2010; 13:133–140. [PubMed: 20023653]

Methods References

29. Rodda SJ, McMahon AP. Distinct roles for Hedgehog and canonical Wnt signaling in specification, differentiation and maintenance of osteoblast progenitors. Development. 2006; 133:3231–3244. [PubMed: 16854976]
30. Logan M, et al. Expression of Cre Recombinase in the developing mouse limb bud driven by a Prxl enhancer. Genesis. 2002; 33:77–80. [PubMed: 12112875]

32. Kisanuki YY, et al. Tie2-Cre transgenic mice: a new model for endothelial cell-lineage analysis in vivo. Developmental biology. 2001; 230:230–242. [PubMed: 11161575]

32. Madisen L, et al. A robust and high-throughput Cre reporting and characterization system for the whole mouse brain. Nat Neurosci. 2010; 13:133–140. [PubMed: 20023653]

33. Lakso M, et al. Efficient in vivo manipulation of mouse genomic sequences at the zygote stage. Proc Natl Acad Sci U S A. 1996; 93:5860–5865. [PubMed: 8650183]

34. Zhang M, et al. Osteoblast-specific knockout of the insulin-like growth factor (IGF) receptor gene reveals an essential role of IGF signaling in bone matrix mineralization. The Journal of biological chemistry. 2002; 277:44005–44012. [PubMed: 12215457]

35. Ara T, et al. A role of CXC chemokine ligand 12/stromal cell-derived factor-1/pre-B cell growth stimulating factor and its receptor CXCR4 in fetal and adult T cell development in vivo. J Immunol. 2003; 170:4649–4655. [PubMed: 12707343]

36. Nagasawa T, et al. Defects of B-cell lymphopoiesis and bone-marrow myelopoiesis in mice lacking the CXC chemokine PBSF/SDF-1. Nature. 1996; 382:635–638. [PubMed: 8757135]

37. Semerad CL, Liu F, Gregory AD, Stumpf K, Link DC. G-CSF is an essential regulator of neutrophil trafficking from the bone marrow to the blood. Immunity. 2002; 17:413–423. [PubMed: 12387736]

38. Churukian C. Lillie's oil red O method for neutral lipids. Journal of Histotechnology. 1999; 4:309–311.

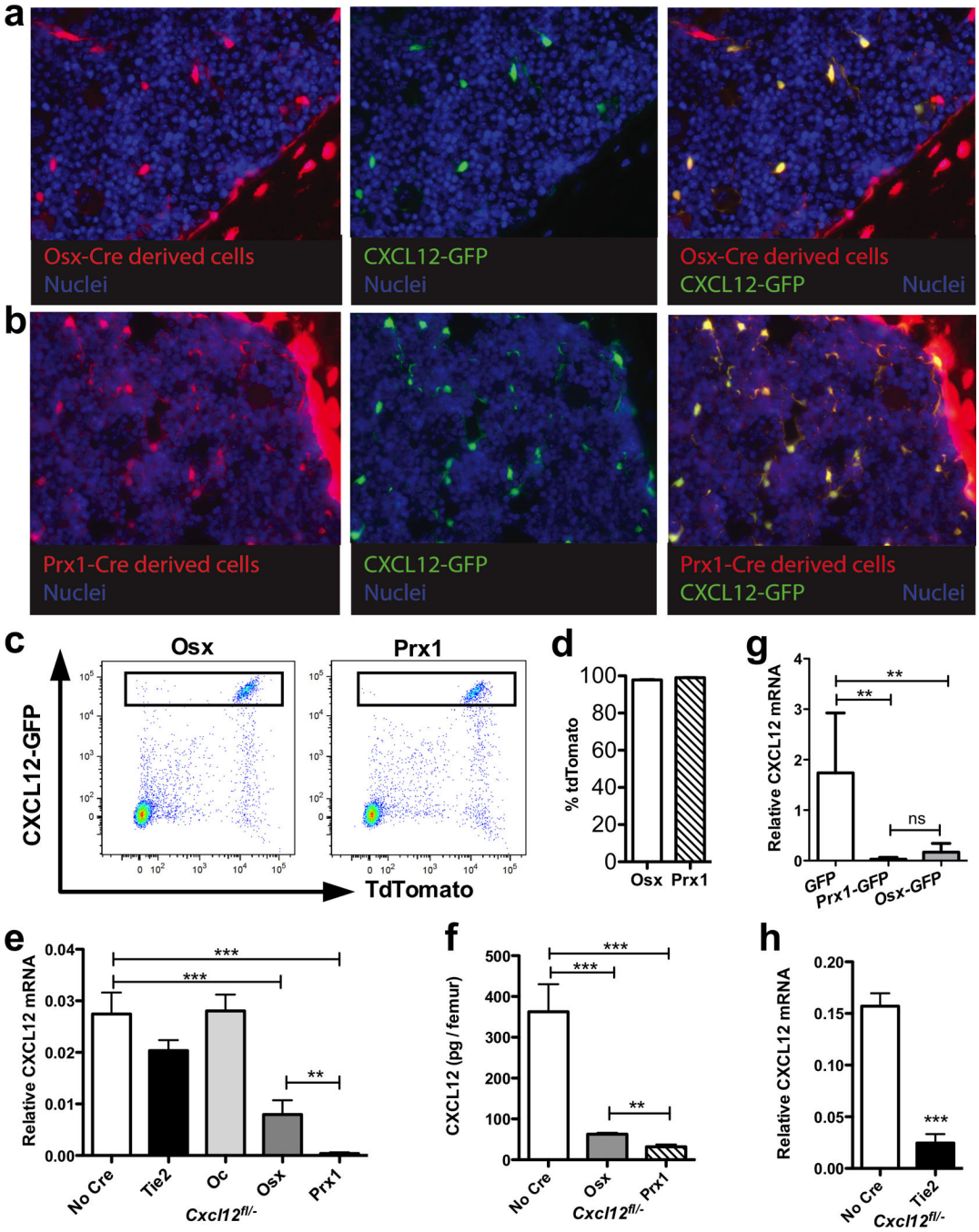

Figure 1. Targeting *Cxcl12* deletion in bone marrow stromal cell populations

Lineage mapping was by performed by generating *Osx-Cre ROSA26*$^{Ai9/+}$ *Cxcl12*$^{gfp/+}$ mice (**a**) or *Prx1-Cre ROSA26*$^{Ai9/+}$ *Cxcl12*$^{gfp/+}$ mice (**b**). Cells that had undergone *Cre*-mediated recombination express tdTomato (red). Cells that express CXCL12 also express GFP (green). Counterstaining with DAPI highlights nuclei (blue). Shown are representative photomicrographs of femur sections. The left panel shows tdTomato fluorescence, the middle panel GFP fluorescence, and the right panel both. Original magnification 40X. (**c**) Representative dot plots showing GFP and tdTomato expression in CD45^{-} lineage^{-} stromal

cells harvested from *Osx-Cre ROSA*$^{Ai9/+}$ *Cxcl12*$^{gfp/+}$ mice (left) or *Prx1-Cre ROSA26*$^{Ai9/+}$ *Cxcl12*$^{gfp/+}$ mice (right). GFP^{bright} CAR cells are boxed. (**d**) Shown is the percentage of CAR cells that express tdTomato (n=5). (**e**) CXCL12 mRNA expression relative to β-actin mRNA is shown on total bone marrow RNA (n=6–13). (**f**) CXCL12 protein in bone marrow extracellular fluid as measured by ELISA (n=3–5). (**g**) CAR cells were sorted from *Osx-Cre Cxcl12*$^{gfp/fl}$ (Osx-GFP), *or Prx1-Cre Cxcl12*$^{gfp/fl}$ (Prx1-GFP*)* mice and RNA prepared. Shown is CXCL12 mRNA expression relative to β-actin mRNA (n=5–7). (**h**) CD31^{+} lineage^{-} CD45^{-} endothelial cells were sorted from *Tie2-Cre*-targeted and control mice, and RNA was prepared. Shown is CXCL12 mRNA expression relative to β-actin mRNA (n=3). *P < 0.05, **P < 0.01; ***P < 0.001.

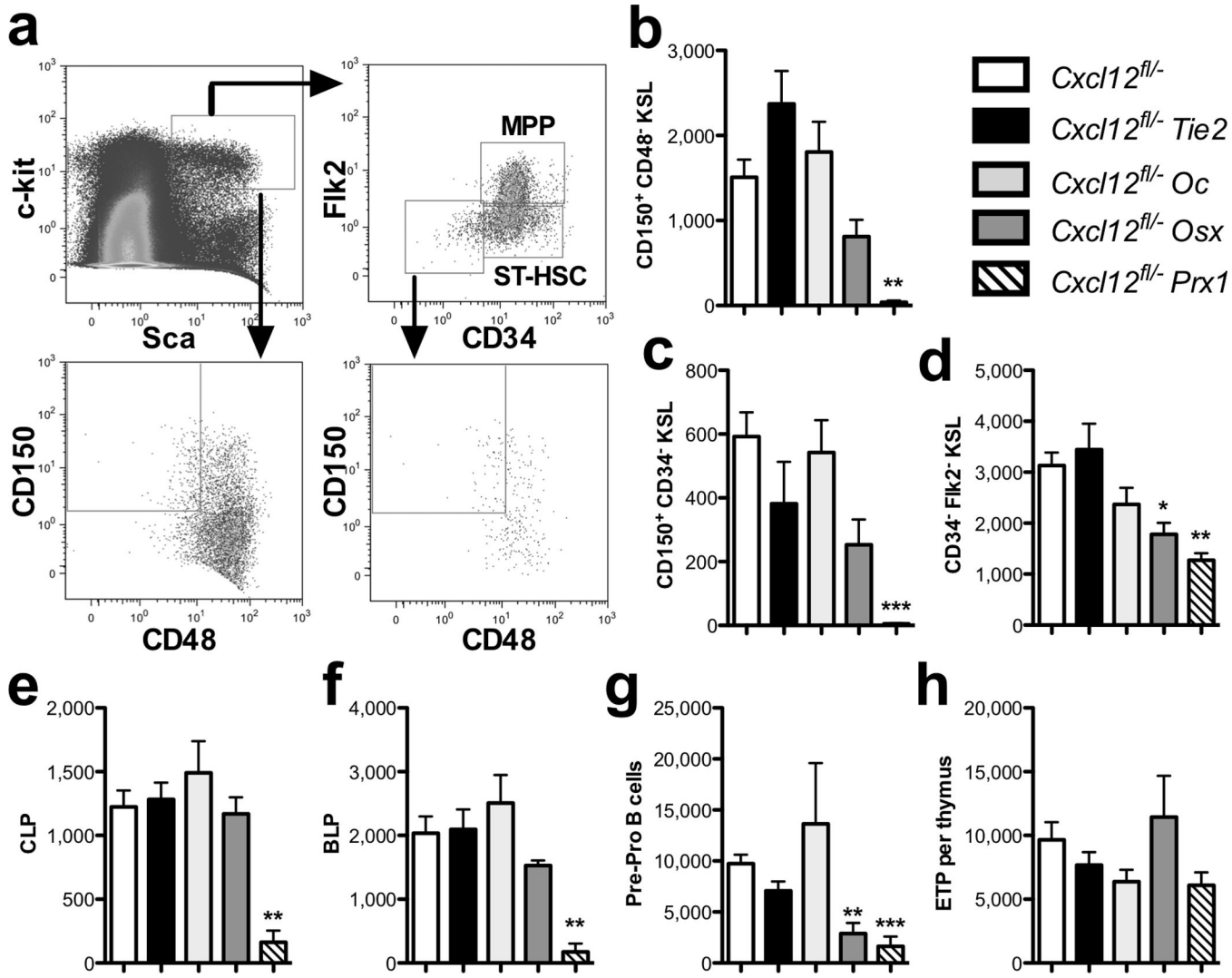

Figure 2. Deletion of *Cxcl12* in defined stromal cell population results in the selective loss of HSCs and lymphoid progenitors

(**a**). Representative dot plots showing the gating strategy to identify HPC populations. Data are gated on lineage$^-$ cells. (**b**) The number of CD150$^+$ CD48$^-$ CD41$^-$ c-Kit$^+$ Sca$^+$ Lineage$^-$ (KSL) cells, (**c**) CD150$^+$ CD41$^-$ CD48$^-$ CD34$^-$ Flk2$^-$ KSL (dormant HSCs), (**d**) CD34$^-$ Flk2$^-$ KSL cells, (**e**) common lymphoid progenitors (CLP), (**f**) B lymphoid progenitors (BLP), and (**g**) pre-pro B cells per femur is shown. (**h**) The number of earliest thymic progenitors (ETP) per thymus is shown. Data represent the mean ± SEM of 6–13 mice. *P < 0.05; **P < 0.01; ***P < 0.001.

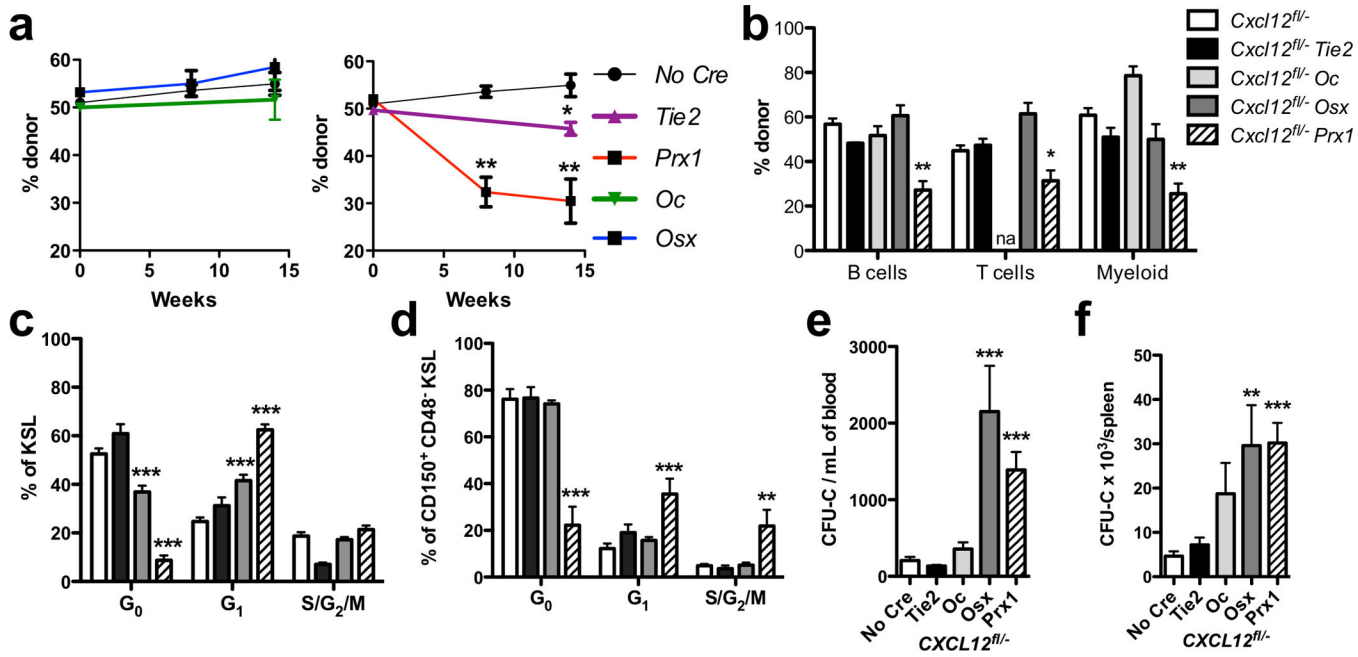

Figure 3. Deletion of *Cxcl12* in defined stromal cell populations results in HPC mobilization and a selective loss of repopulating activity and HSC quiescence

(**a**) Competitive repopulation assays were performed with a one to one ratio of donor and wild-type competitor bone marrow. Shown is the percentage of donor peripheral leukocytes over time. Data represent the mean ± SEM of 10–16 mice. (**b**) The percentage of donor cells in the bone marrow of the indicated lineage 14 weeks after transplantation is shown. Data represent the mean ± SEM of 5–6 mice. (**c & d**) The percentage of cells in the indicated stage of the cell cycle is shown for KSL (**c**) and $CD150^{+}$ $CD48^{-}$ $CD41^{-}$ KSL cells (**d**). The number of colony-forming cells (CFU-C) in the blood (**e**) or spleen (**f**) is shown. Data represent the mean ± SEM of 5–15 mice. *P < 0.05; **P < 0.01; ***P < 0.001. na = not available.

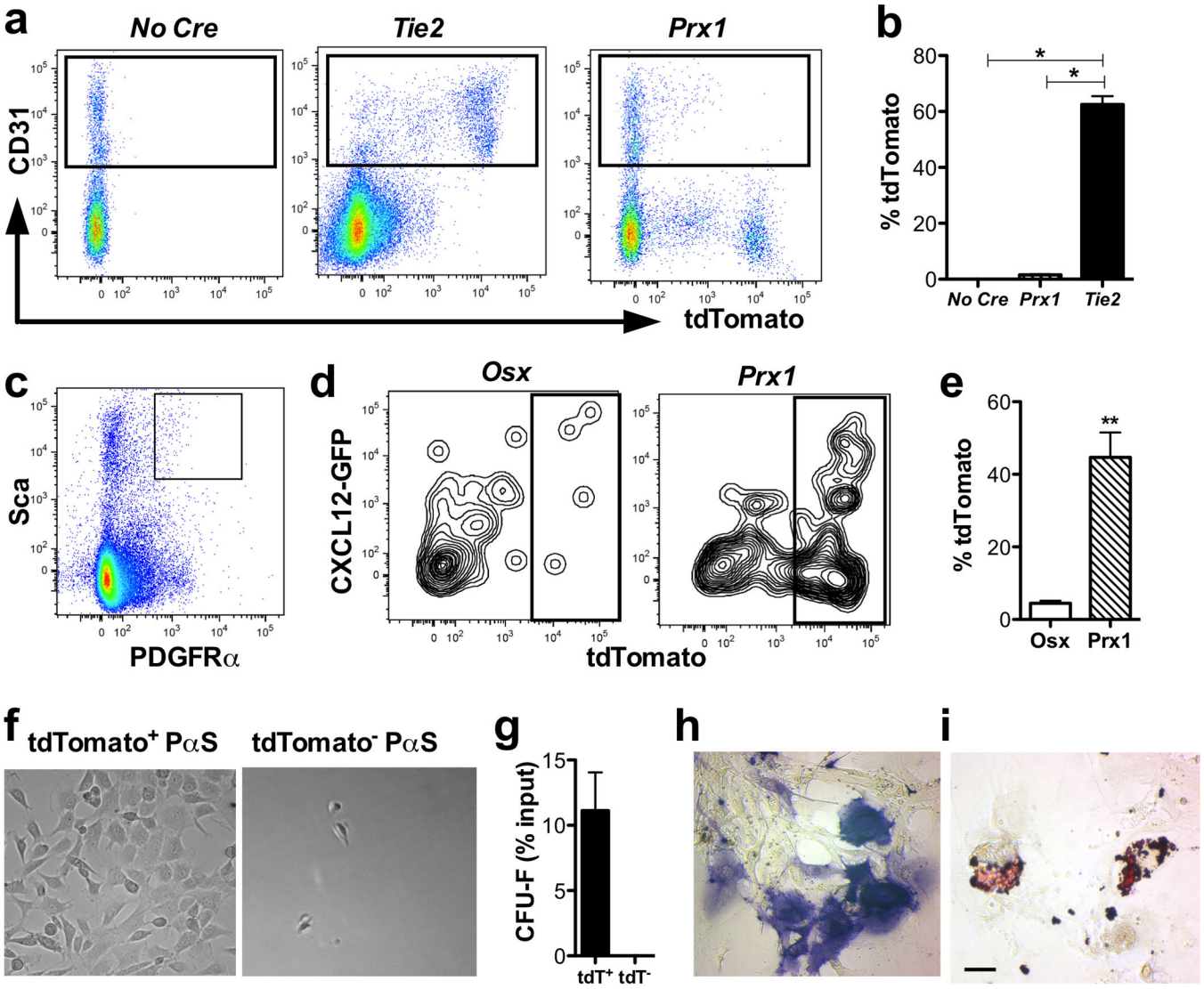

Figure 4. *Prx1-Cre* differentially targets a PDGFRα$^+$ Sca$^+$ CXCL12 expressing mesenchymal progenitor cell population

(**a**) Representative dot plots showing tdTomato and CD31 expression in bone marrow cells from the indicated mice. Data are gated on CD45$^-$ lineage$^-$ cells. (**b**) The percentage of CD31$^+$ CD45$^-$ lineage$^-$ cells that express tdTomato is shown. (**c**) Representative dot plot showing the gating strategy to identify CD45$^-$ lineage$^-$ PDGFRα$^+$ Sca$^+$ cells (boxed). Data are gated on CD45$^-$ lineage$^-$ cells. (**d**) Representative dot plots showing GFP and tdTomato expression in CD45$^-$ lineage$^-$ PDGFRα$^+$ Sca$^+$ (PαS) cells from *Osx-Cre ROSA*$^{Ai9/+}$ *Cxcl12*$^{gfp/+}$ (left panel) or *Prx1-Cre ROSA26*$^{Ai9/+}$ *Cxcl12*$^{gfp/+}$ mice (right panel). (**e**) Shown is the percentage of lineage$^-$ PDGFRα$^+$ Sca$^+$ cells that express tdTomato (n=3). *P < 0.001; **P < 0.01. (**f**) TdTomato$^+$ and tdTomato$^-$ PαS cells were sorted from *Prx1-Cre ROSA26*$^{Ai9/+}$ *Cxcl12*$^{gfp/+}$ mice and colony-forming fibroblast (CFU-F) assays performed. Shown are representative photomicrographs of the cultures on day 14. (**g**) Number of CFU-F per 100 sorted PαS cells. Data represent the mean ± SEM of three independent experiments. Cells were harvested from the CFU-F cultures on day 14 and replated under osteogenic (**h**)

or adipogenic (**i**) culture conditions. Shown are representative photomicrographs of cells stained for alkaline phosphatase or oil red O, respectively. Scale bar = 50 μM.